J. Fluid Mech. (2009), *vol.* 631, *pp.* 363–373.
doi:10.1017/S0022112009007265 Printed in the United Kingdom

Exact solutions for Stokes flow in and around a sphere and between concentric spheres

P. N. SHANKAR†

Computational & Theoretical Fluid Dynamics Division, National Aerospace Laboratories, Bangalore 560 017, India

(Received 24 January 2009 and in revised form 24 March 2009)

A general method is suggested for deriving exact solutions to the Stokes equations in spherical geometries. The method is applied to derive exact solutions for a class of flows in and around a sphere or between concentric spheres, which are generated by meridional driving on the spherical boundaries. The resulting flow fields consist of toroidal eddies or pairs of counter-rotating toroidal eddies. For the concentric sphere case the exact solution when the inner sphere is in instantaneous translation is also derived. Although these solutions are axisymmetric, they can be combined with swirl about a different axis to generate fully three-dimensional fields described exactly by simple formulae. Examples of such complex fields are given. The solutions given here should be useful for, among other things, studying the mixing properties of three-dimensional flows.

1. Introduction

Explicit exact solutions to the field equations have an intrinsic interest of their own. This is especially so if they are for bounded geometries and for flows that are realizable, at least in principle. If their structure is simple they help us, as building blocks, to more clearly visualize more realistic and complex flows. But even apart from this interest, they play a practically useful role, even in these days of much computing power, in helping to check new numerical schemes of computation. This benchmarking role is well appreciated; less well known is that there are certain situations where exact solutions are almost essential, where purely numerical computations are too inaccurate to make reliable progress. An example of the latter is mixing by chaotic advection in laminar flows: any errors in the field calculation can build up exponentially along material lines making mixing calculations unreliable beyond a few periods (Souvaliotis, Jana & Ottino 1995). It is for this reason that so much of our understanding of two-dimensional mixing has had to come from studies of the eccentric annular mixer (Aref & Balachandar 1986; Funakoshi 2008) for which an exact solution exists (Jeffery 1922; Kazakia & Rivlin 1978). Recent progress in the more practical problem of mixing by translating stirrers has been made possible by the discovery of analytical solutions for such motions (Finn & Cox 2001; Cox & Finn 2007).

It is a fact that exact solutions are much harder to compute in three-dimensional geometries and as a consequence are even more valuable. For example Bajer & Moffatt (1990) were able to make use of a general exact solution to first demonstrate

† Email address for correspondence: pn_shankar55@rediffmail.com

chaotic streamlines in a steady bounded three-dimensional flow, that within a sphere. Cartwright, Feingold & Piro (1996), in their analysis of chaotic advection in spherical Couette flow, make use of the leading term in a perturbation solution in Reynolds number found much earlier by Munson & Joseph (1971). The latter had considered viscous swirling flow between concentric rotating spheres and determined the expansion of the field upto the seventh order in Reynolds number.

This paper deals with certain exact solutions for Stokes flow in and around a sphere and between two concentric spheres. We are especially interested here in flows that are caused by meridional driving on the boundaries; for the concentric sphere case, we also deal with given instantaneous translational motion of the inner sphere. The method by which these solutions are derived is discussed in § 2 while the exact solutions are given in § 3. Although these solutions are for axisymmetric flows, they can be combined with a non-coaxial swirl to generate fully three-dimensional flows which are of great interest. Examples of these are briefly considered in § 4.

2. Analysis

Consider steady Stokes flow inside or outside the unit sphere or between two concentric spheres of dimensionless radii 1 and r_0 ($0 < r_0 < 1$), respectively. Suitably normalized governing equations are

$$\nabla \cdot \boldsymbol{u} = 0, \tag{2.1a}$$

$$\nabla^2 \boldsymbol{u} = \nabla p, \tag{2.1b}$$

where $\boldsymbol{u}$ and p are the dimensionless velocity and pressure fields, respectively. It will be convenient to use the Papkovich–Neuber–Imai representation (see Shankar 2007)

$$\boldsymbol{u} = \nabla(\boldsymbol{r} \cdot \boldsymbol{A} + B) - 2\boldsymbol{A} \tag{2.2a}$$

$$p = 2\nabla \cdot \boldsymbol{A} \tag{2.2b}$$

for the field, where $\boldsymbol{A}$ and B are harmonic vector and scalar fields, respectively, and $\boldsymbol{r}$ is the position vector. Although we are interested in generating three-dimensional fields we shall do so by utilizing exact axisymmetric fields. Thus if (r, θ, ϕ) is a spherical polar coordinate system with $\theta = 0$ coinciding with the z-axis of a Cartesian system (x, y, z) with the same origin, we shall seek solutions that are independent of the azimuthal coordinate ϕ.

We will in general be needing both interior eigenfunctions, i.e. those that are regular at the origin, and exterior eigenfunctions, i.e. those that decay at infinity; the former or latter alone will be sufficient for the bare sphere case. In order to utilize representation (2.2) we will need suitable harmonic fields. For the spherical geometry considered here these are given, in another context, in Shankar (2007, § 11.1); and it turns out to be convenient to use the scalar field B and the vector field $\boldsymbol{A}_1$ given there

$$B^i(r, \theta) = r^{n+1} P_{n+1}(\cos\theta), \tag{2.3a}$$

$$\boldsymbol{A}_1^i(r, \theta) = r^n P_n'(\cos\theta)\boldsymbol{e}_\phi, \tag{2.3b}$$

$$B^e(r, \theta) = r^{-n} P_{n-1}(\cos\theta), \tag{2.4a}$$

$$\boldsymbol{A}_1^e(r, \theta) = r^{-n-1} P_n'(\cos\theta)\boldsymbol{e}_\phi. \tag{2.4b}$$

In the above, the superscripts indicate interior and exterior, respectively, the $P_n(\cos\theta)$ are Legendre polynomials and $\boldsymbol{e}_\phi$ is the unit vector in the ϕ-direction. Here and in what follows $P_n'(\cos\theta) = \mathrm{d}P_n(\cos\theta)/\mathrm{d}\theta$. We will however need one more vector field and one is tempted to use the field $\boldsymbol{A}_2$ given in the same source. But, as a referee has pointed out, this leads to formulae that are unnecessarily complicated. Simpler is to use the following harmonic fields suggested by the referee:

$$\boldsymbol{A}_2^i(r,\theta) = r^{n+1}\left\{(n+1)P_n(\cos\theta)\boldsymbol{e}_r - P_n'(\cos\theta)\boldsymbol{e}_\theta\right\}, \tag{2.5a}$$

$$\boldsymbol{A}_2^e(r,\theta) = r^{-n}\left\{nP_n(\cos\theta)\boldsymbol{e}_r + P_n'(\cos\theta)\boldsymbol{e}_\theta\right\}. \tag{2.5b}$$

If we utilize interior and exterior fields (2.3)–(2.5) over the full range of integers n and rearrange indices suitably, we get the following general expansions for the axisymmetric velocity field between two spheres:

$$u_r(r,\theta) = \sum_{n=1}^{\infty}[a_n n r^{n-1} + c_n n(n+1)r^{n+1} - \alpha_n(n+1)r^{-n-2} - \gamma_n n(n+1)r^{-n}]P_n(\cos\theta), \tag{2.6a}$$

$$u_\theta(r,\theta) = \sum_{n=1}^{\infty}[a_n r^{n-1} + c_n(n+3)r^{n+1} + \alpha_n r^{-n-2} + \gamma_n(n-2)r^{-n}]P_n'(\cos\theta), \tag{2.6b}$$

$$u_\phi(r,\theta) = \sum_{n=1}^{\infty}[e_n r^n + \epsilon_n r^{-n-1}]P_n'(\cos\theta), \tag{2.6c}$$

where $a_n, c_n, \alpha_n, \gamma_n, e_n$ and ϵ_n are arbitrary scalars. In future we will drop the argument of the Legendre polynomials with the understanding that it is always $\cos\theta$ and that the prime denotes differentiation with respect to θ. For the case of the containing sphere alone, we will only need the terms involving non-negative powers of r, i.e. in this case $\alpha_n = \gamma_n = \epsilon_n = 0$ for all n; for the exterior problem only the α_n, γ_n and ϵ_n will be needed.

It should be observed that the azimuthal field completely uncouples from the other two components and can be determined independently of them. As they stand, the above expansions can be used to satisfy essentially arbitrary but compatible boundary conditions on the two solid surfaces of the concentric spheres or the single solid surface of a bare sphere, for which the interior or exterior expansions alone will be needed. Note that the (u_r, u_θ) field can be derived from a Stokes stream function Ψ with $u_r = \Psi_{,\theta}/(r^2\sin\theta)$ and $u_\theta = -\Psi_{,r}/(r\sin\theta)$. The stream function corresponding to field (2.6 a, b) is given, up to an arbitrary constant, by

$$\Psi(r,\theta) = -\sum_{n=1}^{\infty}\left[\frac{r^{n+1}}{n+1}a_n + r^{n+3}c_n - \frac{r^{-n}}{n}\alpha_n - r^{-n+2}\gamma_n\right]\sin\theta\,P_n'(\cos\theta). \tag{2.7}$$

Although expansions (2.6) are for general boundary conditions on the solid surfaces of the spheres, our use of them here is for the specialized purpose of generating exact solutions. We derive these by the following method. For some special boundary conditions of simple form, for example with u_r vanishing on the boundaries and say u_θ of the form $\sin j\theta$, we seek the expansion coefficients using the orthogonality properties of the P_n and the expansion of their derivatives in terms of $\sin m\theta$, $m \leqslant j$ (see Lebedev 1972). If the former is used in (2.6a) and the latter in (2.6b) one is led in each case to a simple set of linear algebraic equations for a finite number of coefficients. The

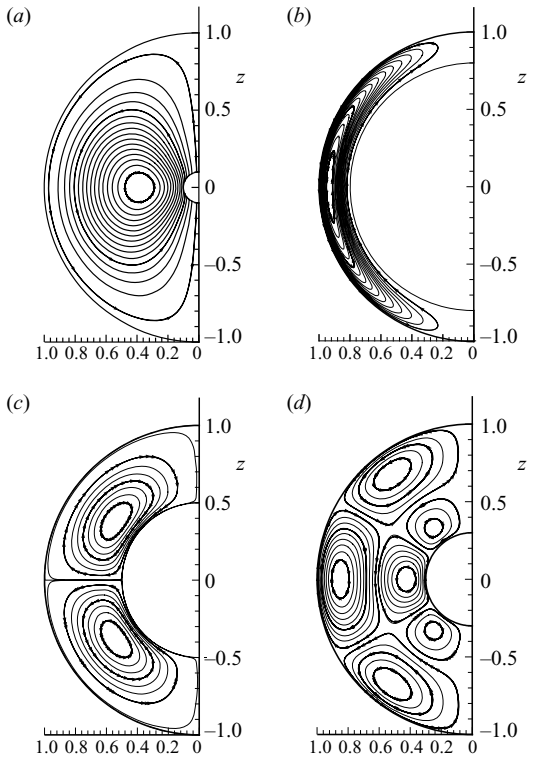

FIGURE 1. Axisymmetric streamline patterns for flows described by exact solutions. (*a*) Inner sphere in instantaneous motion in the z-direction; $r_0 = 0.1$. (*b*)–(*d*) Flows generated by meridional driving as in § 3.2. (*b*) $j = 1$, $r_0 = 0.8$, $V_0 = 0$, $V_1 = 1.0$, (*c*) $j = 2$, $r_0 = 0.5$, $V_0 = 1$, $V_1 = 0$, (*d*) $j = 3$, $r_0 = 0.3$, $V_0 = 3$, $V_1 = 1$.

judicious use of a symbolic manipulation program can help make the calculations quite easy to perform.

3. Exact solutions

3.1. *Inner sphere in uniform motion*

Suppose the inner sphere is instantaneously moving with unit velocity in the z-direction with the outer sphere at rest. Then we just require that $(u_r, u_\theta, u_\phi) = (\cos\theta, -\sin\theta, 0)$ on $r = r_0$ and $\boldsymbol{u} = \boldsymbol{0}$ on $r = 1$. Following the procedure outlined in § 2 we find that the only non-zero expansion coefficients are a_1, c_1, α_1 and γ_1 which are explicitly given by

$$c_1 = 3r_0(1 + r_0)/[2(1 - r_0)^3(4 + 7r_0 + 4r_0^2)], \tag{3.1a}$$

$$\alpha_1 = r_0^3(1 + r_0 + r_0^2)/[(1 - r_0)^3(4 + 7r_0 + 4r_0^2)], \tag{3.1b}$$

$$\gamma_1 = -2c_1 - 3\alpha_1, \tag{3.1c}$$

$$a_1 = \gamma_1 - 4c_1 - \alpha_1. \tag{3.1d}$$

Typical streamlines of this axisymmetric flow field are shown in figure 1(*a*) for the case where $r_0 = 0.1$; not surprisingly, the field consists of a toroidal vortex some of whose streamlines begin and end on the inner sphere.

When considering the simple cases of flows interior or exterior to a single sphere, the sphere will be taken to be of unit radius and the velocity scales the one associated with that sphere. In the case of a single sphere moving in the z-direction the only non-zero coefficients are

$$\alpha_1 = 1/4 \tag{3.2a}$$

$$\gamma_1 = -3/4 \tag{3.2b}$$

consistent with the well-known formula for Stokes flow around a moving sphere (Batchelor 1967, equation (4.9.12)).

3.2. *Meridional driving on the inner and outer boundaries*

The exact solutions considered here deal with situations where the fluid is driven by meridional driving on the spherical boundaries. Specifically we consider axisymmetric flows where the boundary conditions take the form

$$u_r(r_0, \theta) = 0, \tag{3.3a}$$

$$u_r(1, \theta) = 0, \tag{3.3b}$$

$$u_\theta(r_0, \theta) = V_0 \sin j\theta, \tag{3.4a}$$

$$u_\theta(1, \theta) = V_1 \sin j\theta, \tag{3.4b}$$

where j is an integer. The motivation for the above assumed form is that it is precisely such a form with $j = 1$ that appears in Bajer & Moffatt (1990, equation (2.7)) and with $j = 2$ that appears in Cartwright *et al.* (1996, equation (3.16)). The exact solutions for the cases $j = 1$, 2, 3 and 4 are as follows:

3.2.1. *Case* $j = 1$

We find in this case also that the only non-zero expansion coefficients are a_1, c_1, α_1 and γ_1. However they are now given by

$$c_1 = -[V_1(2 + r_0) + V_0(r_0 + 2r_0^2)]/[(1 - r_0)^2(4 + 7r_0 + 4r_0^2)], \tag{3.5a}$$

$$\alpha_1 = -r_0^3[V_1(1 + 2r_0) + V_0(2 + r_0)]/[(1 - r_0)^2(4 + 7r_0 + 4r_0^2)], \tag{3.5b}$$

$$\gamma_1 = -V_1 - 2c_1 - 3\alpha_1, \tag{3.5c}$$

$$a_1 = 2\gamma_1 + 2\alpha_1 - 2c_1. \tag{3.5d}$$

Streamline patterns when $r_0 = 0.8$, $V_1 = 1$ and $V_0 = 0$ are shown in figure 1(b). Now we have a single toroidal eddy, symmetrically placed about $z = 0$, all of whose streamlines are closed.

For flow in a sphere the only non-zero coefficients are

$$a_1 = 1, \tag{3.6a}$$

$$c_1 = -1/2. \tag{3.6b}$$

The streamlines are those due to a single toroidal eddy as above. Note that (3.6) is in agreement with (2.7) of Bajer & Moffatt (1990). For the exterior flow the only non-zero coefficients are $\alpha_1 = -\gamma_1 = -1/2$.

3.2.2. *Case* $j = 2$

In this case the only non-zero expansion coefficients are a_2, c_2, α_2 and γ_2. Let

$$D = (1 - r_0)^2(4 + 16r_0 + 40r_0^2 + 55r_0^3 + 40r_0^4 + 16r_0^5 + 4r_0^6). \tag{3.7}$$

Then the non-zero coefficients are given by

$$c_2 = -2[V_1(2 + 4r_0 + 6r_0^2 + 3r_0^3) + V_0 r_0^2(3 + 6r_0 + 4r_0^2 + 2r_0^3)]/(3D), \tag{3.8a}$$

$$\alpha_2 = -4r_0^4[V_1 r_0(3 + 6r_0 + 4r_0^2 + 2r_0^3) + V_0(2 + 4r_0 + 6r_0^2 + 3r_0^3)]/(3D), \tag{3.8b}$$

$$a_2 = -2V_1/3 - \alpha_2 - 5c_2, \tag{3.8c}$$

$$\gamma_2 = (2a_2 + 6c_2 - 3\alpha_2)/6. \tag{3.8d}$$

Figure 1(*c*) shows typical streamlines when $r_0 = 0.5$, $V_0 = 1$ and $V_1 = 0$. There are two axisymmetric toroidal eddies, symmetrically placed above and below $z = 0$; all the streamlines are closed.

The only non-zero coefficients in the internal sphere are

$$a_2 = 1, \tag{3.9a}$$

$$c_2 = -1/3. \tag{3.9b}$$

As in the concentric spheres case the field consists of two toroidal eddies. For the exterior flow the only non-zero coefficients are $\alpha_2 = -2/3$ and $\gamma_2 = 1/3$.

3.2.3. *Case* $j = 3$

Now the only non-zero expansion coefficients are $a_1, c_1, \alpha_1, \gamma_1, a_3, c_3, \alpha_3$ and γ_3. Let

$$D = (1 - r_0)^2(4 + 16r_0 + 40r_0^2 + 80r_0^3 + 140r_0^4 + 175r_0^5 + 140r_0^6 + 80r_0^7 + 40r_0^8 + 16r_0^9 + 4r_0^{10}) \tag{3.10}$$

Then α_3 and γ_3 are given by

$$\alpha_3 = -8r_0^5[V_1 r_0^2(5 + 10r_0 + 8r_0^2 + 6r_0^3 + 4r_0^4 + 2r_0^5) + V_0(2 + 4r_0 + 6r_0^2 + 8r_0^3 + 10r_0^4 + 5r_0^5)]/(5D), \tag{3.11a}$$

$$\gamma_3 = 8r_0^3[V_1 r_0^2(7 + 14r_0 + 12r_0^2 + 10r_0^3 + 8r_0^4 + 6r_0^5 + 4r_0^6 + 2r_0^7) + V_0(2 + 4r_0 + 6r_0^2 + 8r_0^3 + 10r_0^4 + 12r_0^5 + 14r_0^6 + 7r_0^7]/(15D). \tag{3.11b}$$

It follows then that

$$a_3 = 6\alpha_3 + 14\gamma_3 + 16V_1/15, \tag{3.12a}$$

$$c_3 = -(a_3 + \alpha_3 + \gamma_3 + 8V_1/15)/6. \tag{3.12b}$$

The $n = 1$ terms can be uncoupled and solved to give

$$\alpha_1 = r_0^3 \frac{V_1(1 + 2r_0) + V_0(2 + r_0)}{5(1 - r_0)^2(4 + 7r_0 + 4r_0^2)}, \tag{3.13a}$$

$$\gamma_1 = -r_0 \frac{V_1(3 + 6r_0 + 4r_0^2 + 2r_0^3) + V_0(2 + 4r_0 + 6r_0^2 + 3r_0^3)}{5(1 - r_0)^2(4 + 7r_0 + 4r_0^2)}, \tag{3.13b}$$

$$c_1 = \frac{(1 - r_0^{-3})\alpha_1 + (1 - r_0^{-1})\gamma_1}{1 - r_0^2}, \tag{3.13c}$$

$$a_1 = 2(-c_1 + \alpha_1 + \gamma_1). \tag{3.13d}$$

Streamline patterns for this case are shown in figure 1(*d*) when $r_0 = 0.3$, $V_0 = 3$ and $V_1 = 1$. Now, since there is meridional driving in the same direction on both surfaces, we have three pairs of counter-rotating toroidal eddies. All the streamlines are closed.

For the spherical container alone the only significant coefficients are

$$a_1 = -1/5, \tag{3.14a}$$
$$c_1 = 1/10, \tag{3.14b}$$
$$a_3 = 16/15, \tag{3.14c}$$
$$c_3 = -4/15. \tag{3.14d}$$

The field consists of three toroidal eddies. For the exterior problem the non-zero coefficients are $\alpha_1 = -\gamma_1 = 1/10$, $\alpha_3 = -4/5$ and $\gamma_3 = 4/15$.

3.2.4. *Case* $j = 4$

The only non-zero coefficients now are $a_2, c_2, \alpha_2, \gamma_2, a_4, c_4, \alpha_4$ and γ_4. Let

$$D = (1-r_0)^2(4 + 16r_0 + 40r_0^2 + 80r_0^3 + 140r_0^4 + 224r_0^5 + 336r_0^6 + 399r_0^7 + 336r_0^8 + 224r_0^9 + 140r_0^{10} + 80r_0^{11} + 40r_0^{12} + 16r_0^{13} + 4r_0^{14}). \tag{3.15}$$

Then

$$\alpha_4 = -64r_0^6[V_1 r_0^3(7 + 14r_0 + 12r_0^2 + 10r_0^3 + 8r_0^4 + 6r_0^5 + 4r_0^6 + 2r_0^7) + V_0(2 + 4r_0 + 6r_0^2 + 8r_0^3 + 10r_0^4 + 12r_0^5 + 14r_0^6 + 7r_0^7)]/(35D), \tag{3.16a}$$

$$\gamma_4 = 16r_0^4[V_1 r_0^3(9 + 18r_0 + 16r_0^2 + 14r_0^3 + 12r_0^4 + 10r_0^5 + 8r_0^6 + 6r_0^7 + 4r_0^8 + 2r_0^9) + V_0(2 + 4r_0 + 6r_0^2 + 8r_0^3 + 10r_0^4 + 12r_0^5 + 14r_0^6 + 16r_0^7 + 18r_0^8 + 9r_0^9)]/(35D), \tag{3.16b}$$

$$c_4 = -(9\alpha_4 + 28\gamma_4 + 64V_1/35)/8, \tag{3.16c}$$
$$a_4 = -(7c_4 + \alpha_4 + 2\gamma_4 + 16V_1/35). \tag{3.16d}$$

If now

$$D = (1-r_0)^2(4 + 16r_0 + 40r_0^2 + 55r_0^3 + 40r_0^4 + 16r_0^5 + 4r_0^6), \tag{3.17}$$

the $n = 2$ terms uncouple and are given by

$$\alpha_2 = 8r_0^4[V_1 r_0(3 + 6r_0 + 4r_0^2 + 2r_0^3) + V_0(2 + 4r_0 + 6r_0^2 + 3r_0^3)]/(21D), \tag{3.18a}$$

$$\gamma_2 = -4r_0^2[V_1 r_0(5 + 10r_0 + 8r_0^2 + 6r_0^3 + 4r_0^4 + 2r_0^5) + V_0(2 + 4r_0 + 6r_0^2 + 8r_0^3 + 10r_0^4 + 5r_0^5)]/(21D), \tag{3.18b}$$

$$c_2 = [(r_0 - r_0^{-4})\alpha_2 + 2(r_0 - r_0^{-2})\gamma_2]/[2(r_0 - r_0^3)], \tag{3.18c}$$
$$a_2 = (-6c_2 + 3\alpha_2 + 6\gamma_2)/2. \tag{3.18d}$$

Naturally, the field in this case will consist of either four eddies if there is driving on only one boundary or of four pairs of counter-rotating eddies in case there is driving in the same direction on both boundaries.

For the spherical container alone the only non-zero coefficients are

$$a_2 = -2/7 \tag{3.19a}$$
$$c_2 = 2/21 \tag{3.19b}$$
$$a_4 = 8/7 \tag{3.19c}$$
$$c_4 = -8/35 \tag{3.19d}$$

while for the exterior problem the non-zero coefficients are $\alpha_2 = 4/21$, $\gamma_2 = -2/21$, $\alpha_4 = -32/35$ and $\gamma_4 = 8/35$.

It is clear from the four cases discussed above that in general exact solutions exist for every integer value of j. That for each j one will have either j or $2j$ toroidal

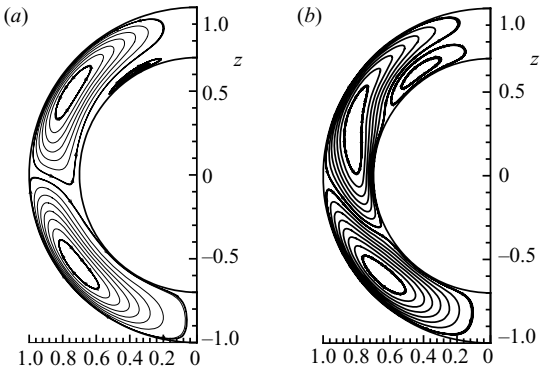

FIGURE 2. Meridionally driven flows with different driving protocols on the two surfaces. $r_0 = 0.7$, $V_1 = 1$, $j_0 = 3$, $j_1 = 2$. (*a*) $V_0 = 0.1$ and (*b*) $V_0 = 0.5$.

eddies depending on whether driving is on a single boundary or on both in the same direction. From the way the calculations proceed and the general pattern of the non-zero coefficients found above, one can state the form of their distribution for the general case. For the concentric sphere case, for even j, the overall pattern is of the form $\{a_j, c_j, \alpha_j, \gamma_j, a_{j-2}, c_{j-2}, \alpha_{j-2}, \gamma_{j-2}, \ldots, a_2, c_2, \alpha_2, \gamma_2\}$; for odd j the pattern is of the form $\{a_j, c_j, \alpha_j, \gamma_j, a_{j-2}, c_{j-2}, \alpha_{j-2}, \gamma_{j-2}, \ldots, a_1, c_1, \alpha_1, \gamma_1\}$. The patterns for the interior and exterior problems of a single sphere follow immediately.

It should be noted that one can handle the situation where the meridional components on the spheres are of the form $\sin j_0\theta$ and $\sin j_1\theta$, respectively, on the two spheres, with $j_0 \neq j_1$. All one needs to do is to superpose the solutions of the two individual cases with a non-zero meridional component on only one of the spheres. Figure 2 shows two such flows, differing only in the intensity of the inner driving, for the case where $j_0 = 3$ and $j_1 = 2$. If the driving protocols had been the same, one would have had either two pairs of counter-rotating eddies or three such pairs, as in figure 1(*d*). Now, however, there is considerable distortion of the eddy structure with no symmetry about the x–y plane. When V_0 is relatively small as in figure 2(*a*) the outer flow, with two toroidal eddies, dominates; however, even in this case there is a single counter-rotating eddy on the upper part of the inner sphere. Consideration of the driving on the inner sphere shows that the other two eddies normally adjacent to it cooperate with the outer flow and are subsumed by it. With increasing V_0, as in figure 2(*b*), the distortion increases with, however, the number of eddies remaining in the same. With further increases in V_0 so that $V_0 \gg V_1$, the field behaves as if the driving was on the inner sphere alone with the outer field only tending to distort the field slightly.

3.3. *Pure swirl about the z-axis*

Finally, we consider the case where the inner and outer spheres rotate about the z-axis with angular speeds ω_0 and ω_1, respectively, i.e. $\boldsymbol{u}(r_0, \theta) = (0, 0, \omega_0 r_0 \sin\theta)$ and $\boldsymbol{u}(1, \theta) = (0, 0, \omega_1 \sin\theta)$. Now only expansion (2.6*c*) is needed and it trivially follows that the field is given by

$$u_\phi(r, \theta) = \sin\theta \left[(\omega_1 - r_0^3\omega_0)r - r_0^3(\omega_1 - \omega_0)r^{-2}\right]/(1 - r_0^3). \tag{3.20}$$

This result is well known (see for example Munson & Joseph 1971).

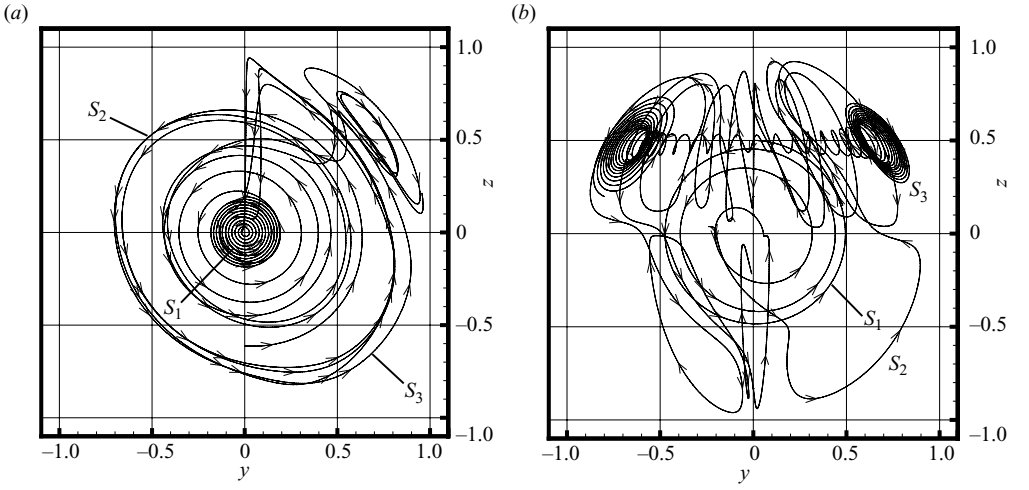

FIGURE 3. Three-dimensional streamline patterns in flows generated by superposing, on meridional flows, a swirling flow whose axis is at 90° to the z-axis. The views seen are of three streamlines in each case as seen along the x-axis, i.e. the swirl axis. $j=2$, $r_0=0.5$, $V_0=0$, $\omega_0=1$, $\omega_1=0$. (*a*) $V_1=0.1$ and (*b*) $V_1=5/3$.

4. Discussion and conclusion

The exact solutions that have been obtained in § 3 are for axisymmetric flow fields generated by axisymmetric boundary conditions. However our primary interest is in fully three-dimensional flows. But as Cartwright *et al.* (1996) have shown it is possible to generate complex three-dimensional fields by superposing axisymmetric fields which are not coaxial. Such a superposition is possible because of the linearity of the Stokes equations and the use of a concentric geometry. We will briefly illustrate such a use of the exact solutions with a simple example.

Consider concentric spheres subjected to meridional forcing of the type considered in § 3.2. Let us superpose on this flow a purely swirling flow of the type considered in § 3.3 but we now have the swirl taken place about an axis that is tilted at an angle α to the z-axis. It is immediately clear that for $\alpha \neq 0, \pi$ the composite flow field will be fully three-dimensional. Since both the primary meridional field and the swirling flow are given by simple exact solutions, the three-dimensional field is now described by simple exact formulae involving the finite expansions and a coordinate transformation. Figure 3 shows two such three-dimensional flow fields generated by meridional forcing of the type $\sin 2\theta$ together with swirl about an axis at 90° to the z-axis. The tilt angle has been chosen so that it will be comparatively easy to visualize what is happening. In both cases $r_0=0.5$, $V_0=0$, $\omega_1=0$, $\omega_0=1$, the only difference being that $V_1=0.1$ in figure 3(*a*) but is 5/3 in figure 3(*b*), i.e. the meridional flow is of much greater intensity in the latter.

Note that in both figures 3(*a*) and 3(*b*) the view is in the x-direction, i.e. along the direction of the swirl, and what is seen are three streamlines each passing through the same three points. The streamlines s_1, s_2 and s_3 pass through the points with (x, y, z) coordinates (0.51, 0.0, 0.01), (0.9, 0.0, 0.2) and (0.7, 0.0, 0.5), respectively. Note that if V_1 had been 0 all the streamlines would be the closed circles of pure swirling flow; if ω_1 had been 0 the streamlines would be similar to those seen in figure 1(*c*). Although it is difficult from this view alone to see what is happening, other views show that

although the swirl is the strong primary flow in figure 3(a), the effect of the weak meridional component is inexorable. Rather then having closed circular paths, the streamlines near the inner sphere begin to diverge outwards and as they do so they increasingly come under the influence of the meridional flow. But the nature of the meridional flow is such that near the poles the flow weakens and the influence of the swirl once again takes over. This is why one sees all three streamlines in figure 3(a) move downwards and into the swirl near the plane $y = 0$. Note that s_1 is most strongly influenced by the swirl as the starting location has been chosen suitably. On the other hand both s_2 and s_3, unlike s_1, have two loops in the meridional motion seen on the upper right of the figure.

The situation is quite different in figure 3(b). Here the meridional motion is comparable in magnitude to the swirling motion near the inner sphere. Note that s_1 is now not tightly wound around the x-axis because the meridional flow now influences it much more; and although it cannot be seen in this view there are now loops in the meridional field. The second streamline now makes many loops in the meridional field while s_3 now most dramatically forms a part of the vortex that starts and ends on the plane $x = 0$. Note that when $\alpha = 90^\circ$ the field is made up of two non-interacting parts on either side of this plane. Since our primary purpose was to derive the exact solutions and show how they can be used, we do not examine these interesting fields in any detail.

We conclude by pointing out that whereas the flows in or outside the sphere alone do not depend, following non-dimensionalization, on any parameter, the flows between concentric spheres involve two parameters, a ratio of length scales r_0 and a ratio of velocity scales V_0/V_1 (or its inverse). As a consequence these flow fields should be useful in validating numerical schemes over a large parameter space. The other use that we can immediately foresee is in studying the mixing properties of three-dimensional flows, again over a large parameter space.

I would like to acknowledge the Council of Scientific & Industrial Research for an award in its Emeritus Scientist scheme and the National Aerospace Laboratories for its continuing support. Grateful thanks are to Ranga Kidambi for some valuable suggestions, D. Shobha and Josy Pullockara for help with the manuscript preparation and to a referee for a suggestion that greatly simplified these calculations.

REFERENCES

Aref, H. & Balachandar, S. 1986 Chaotic advection in a Stokes flow. *Phys. Fluids* **29**, 3515–3521.

Bajer, K. & Moffatt, H. K. 1990 On a class of steady confined Stokes flows with chaotic streamlines. *J. Fluid Mech.* **212**, 337–363.

Batchelor, G. K. 1967 *An Introduction to Fluid Dynamics*. Cambridge.

Cartwright, J. H. E., Feingold, M. & Piro, O. 1996 Chaotic advection in three-dimensional unsteady incompressible laminar flow. *J. Fluid Mech.* **316**, 259–284.

Cox, S. M. & Finn, M. D. 2007 Two-dimensional Stokes flow driven by elliptical paddles. *Phys. Fluids* **19**, 113102.

Finn, M. D. & Cox, S. M. 2001 Stokes flow in a mixer with changing geometry. *J. Engng Math.* **41**, 75–99.

Funakoshi, M. 2008 Chaotic mixing and mixing efficiency in a short time. *Fluid Dyn. Res.* **40**, 1–33.

Jeffery, G. B. 1922 The rotation of two circular cylinders in a viscous fluid. *Proc. R. Soc. Lond.* **101**, 169–174.

Kazakia, J. Y. & Rivlin, R. S. 1978 Flow of a Newtonian fluid between eccentric rotating cylinders and related problems. *Stud. Appl. Math.* **58**, 209–247.

Lebedev, N. N. 1972 *Special Functions and Their Applications*. Dover.

Munson, B. R. & Joseph, D. D. 1971 Viscous incompressible flow between concentric rotating spheres. Part 1. Basic flow. *J. Fluid Mech.* **49**, 289–303.

Shankar, P. N. 2007 *Slow Viscous Flows – Qualitative Features and Quantitative Analysis Using the Method of Complex Eigenfunction Expansions*. Imperial College Press.

Souvaliotis, A., Jana, S. C. & Ottino, J. M. 1995 Potentialities and limitations of mixing simulations. *AIChE J.* **41**, 1605–1621.